*Original Article*

**SAGE Open Medicine**

SAGE Open Medicine
Volume 6: 1–12

DOI: 10.1177/2050312118783412
journals.sagepub.com/home/smo
SAGE

# Modulation of endoplasmic reticulum stress and the unfolded protein response in cancerous and noncancerous cells

**Marcy C Purnell[1,2], Matthew BA Butawan[3], Kemal Bingol[1], Elizabeth A Tolley[4], and Michael A Whitt[1]**

## Abstract

**Objectives:** The bio-field array is a device that generates a dielectrophoretic electromagnetic field when placed in a hypotonic saline solution and a direct current of approximately 3 A is applied. It is known that cell physiology is guided by bioelectrical properties, and there is a significant growth inhibition in cancerous (MDA-MB-231) cells that are grown in media that has been reconstituted with the saline that has been exposed to the bio-field array direct current dielectrophoretic electromagnetic field, alternatively there is no growth inhibition noted in noncancerous cells (MCF-10A) when grown in the bio-field array direct current dielectrophoretic electromagnetic field treated versus control media.

**Methods:** To examine the basis for selective growth inhibition in human breast carcinoma, we employed cell death assays, cell cycle assays, microarray analysis and reverse transcription-quantitative polymerase chain reaction.

**Results:** We found a large transcriptional reprogramming in the cell lines and of the genes affected, those involved in endoplasmic reticulum stress and the unfolded protein response pathways showed some of the most dramatic changes. Cancerous cells grown in media that has been reconstituted with a hypotonic saline solution that has been exposed to the bio-field array direct current dielectrophoretic electromagnetic field show a significant and strong upregulation of the apoptotic arms of the unfolded protein response while the noncancerous cells show a decrease in endoplasmic reticulum stress via microarray analyses and reverse transcription-quantitative polymerase chain reaction.

**Conclusion:** The bio-field array shows potential to initiate apoptosis in cancerous cells while relieving cell stress in noncancerous cells in vitro. These studies lay a foundation for nurses to conduct future in vivo models for the possible development of future adjunct treatments in chronic disease.

## Keywords

Cancer growth, apoptosis, endoplasmic reticulum stress, unfolded protein response, microarray analysis

Date received: 17 April 2018; accepted: 25 May 2018

## Introduction

The endoplasmic reticulum (ER) plays a key role in protein biosynthesis and protein folding in a cell.[1] Polypeptide chains must be appropriately folded into their signature quaternary or tertiary structures to be recognized and utilized by the cell/organism.[2] When the ER begins to struggle with the folding of proteins due to intracellular changes, micro-environmental changes, high-fat or high-sugar exposure, certain prescription drugs and so on, misfolded proteins begin to accumulate in the ER and activation of the unfolded protein response (UPR) occurs.[1] The UPR is a rescue/repair mechanism of a cell that initiates (a) the halting of protein translation, (b) the degrading of misfolded proteins, (c) the activation of chaperones/heat shock proteins to assist with the misfolded protein accumulation, and (d) cell cycle arrest.[3] If these rescue mechanisms do not relieve the ER stress due to the accumulation of misfolded proteins within an appropriate time frame, the pro-apoptotic

[1]Department of Microbiology, Immunology and Biochemistry, College of Medicine, The University of Tennessee Health Science Center, Memphis, TN, USA
[2]The Loewenberg College of Nursing, The University of Memphis, Memphis, TN, USA
[3]School of Health Studies, The University of Memphis, Memphis, TN, USA
[4]Department of Preventive Medicine, The University of Tennessee Health Science Center, Memphis, TN, USA

**Corresponding author:**
Marcy C Purnell, The Loewenberg College of Nursing, The University of Memphis, Memphis, TN 38152, USA.
Email: mpurnell@memphis.edu

arm is activated and the cell initiates cell death through apoptosis. This cell death initiation has been implicated in neurodegenerative, metabolic and inflammatory diseases.[3] Also, cancer cells can use this pathway to prevent the appropriate response to normal growth signaling by hijacking chaperone upregulation that occurs during the UPR.[4] This allows cancer cells to continue to fold specific proteins needed for unchecked mitosis.[4]

The studies described here utilized a device called the bio-field array (BFA) that generates a direct current (dc)-driven, dielectrophoretic (DEP) electromagnetic field (EMF) in dilute saline solutions.[5–7] This device was developed in Australia in 1996 (patent no.: US6555071; published patent no.: US 2017/0232253 A1) and has been sold in alternative health markets as a footbath. It consists of a power supply that converts alternating current (ac) to dc and delivers 3.0 A of this dc to an array of conductive rings and creates a magnetic behavioral change in the chloride ions through a DEP disassociation of the metal aqueous ions in a hypotonic saline solution.[5] Dielectrophoresis (versus simple electrolysis) occurs when a force (such as dc) is exerted on and changes the polarity of a dielectric particle (such as a chloride ion) in a non-uniform electric field.[5,8] When a dielectric particle is separated from other molecules in a DEP field, it does not conduct electricity but instead it exhibits a polarity change (ferroelectricity).[5,9] Our data suggest that the diamagnetic (dielectric) chloride ion changes polarity in the BFA dc-DEP-EMF and appears to orient and interact with the membrane in such a way that leads to significant increase in chloride ion channel activity and possibly a more bioavailable form we have termed biochloride ($_bCl^-$).[5,10]

Individuals use the BFA device by submerging their hands, feet, or entire body in water while dc is applied to the array (that is placed in the water) via the dc converter power supply. In order to determine if this technology and the associated consumer-based anecdotal reports of health benefits could be correlated to any experimental and gene expression changes, we performed in vitro studies to quantify any possible changes in cell physiology and gene expression profiles (Supplementary Tables S1 and S2). We employed this in vitro modeling to obtain pre-clinical data for possible in vivo models and human trials. The in vitro experiments were conducted with an aggressive human breast cancerous cell line (MDA-MB-231 human triple-negative cancer—which is not likely to respond to hormonal therapies) and a noncancerous epithelial cell line (MCF-10A—control). These experiments were to investigate the mechanisms of action at the cellular level that could explain the significant growth inhibition of this cancerous cell line that was noted in the initial pilot studies.[5,7] Here, we will discuss the significant findings from our in vitro studies that have served as preliminary data for designing and conducting our current in vivo and human studies that are underway to investigate the potential of this technology as a future, holistic and non-invasive adjunct treatment for chronic disease that could be pioneered by nursing in collaboration with other medical professionals.[11]

## Methods and materials

### Cells growth prior to analyses

Human MDA-MB-231 triple-negative breast carcinoma and human MCF-10A breast epithelial cells were obtained from the American Type Culture Collection (ATCC). The MDA-MB-231 cells were maintained in high-glucose Dulbecco's Modified Eagles Medium (DMEM, Lonza #12-604Q) containing 10% fetal bovine serum (FBS; Atlanta Biologicals). MCF-10A cells were maintained in DMEM/F12 (Invitrogen cat. #11330-032) supplemented with 20 ng/ml epidermal growth factor (PeproTech cat. #100-47), 0.5 mg/ml hydrocortisone (Sigma-Aldrich cat. #H-0888), 100 ng/ml cholera toxin (Sigma-Aldrich cat. #C-8052), 10 μg/ml insulin (Sigma-Aldrich cat. #I-1882) and 5% horse serum (Invitrogen cat. #11330-032).

To prepare dc-DEP-EMF–treated and control DMEM, 10X DMEM (Sigma cat. #D2429) was diluted 9:1 with a hypotonic saline solution that had been treated for 30 min at 2 A of dc with the BFA device or with an aliquot of the same solution prior to treatment with the device. The hypotonic saline solution consisted of 3 mM NaCl prepared using laboratory-grade deionized water and molecular biology-grade NaCl (Promega cat. #V4221). Complete treated and control DMEM was supplemented with 0.004 gm/l of folic acid (Sigma-Aldrich cat. #F8758-5G), 4000 mg/l of glucose (Sigma-Aldrich cat. G7021-100G), 0.584 gm/l of glutamine (Sigma-Aldrich cat. #G7513), and 3.7 gm/l of sodium bicarbonate (BioWhittaker cat. #15-6131) and filtered through a 0.22-μm-pore sized bottle top filter (Corning cat. #430624). FBS was then added to 10% final concentration.

To prepare treated and control media for the growth of MCF-10A cells, F-12 nutrient mix powder (Life technologies cat. #21700-026) was re-suspended in either BFA dc-DEP-EMF-treated saline, or with an aliquot of the same solution prior to treatment with the device. The F-12 media was then mixed 1:1 with DMEM prepared as described above with either BFA-treated or control saline and then the DMEM/F12 was supplemented with epidermal growth factor (EGF), cholera toxin and insulin as described above and then filter sterilized as described above. Horse serum was then added to 5% final concentration.

For the BFA-treated and control groups, aliquots of 10,000 cells were seeded into three 6-well plates for each of the two groups and for each cell line using media purchased from commercial vendors and supplemented with either FBS or horse serum. The next day the media were replaced with freshly prepared BFA-treated or control media until the cells were removed for cell cycle microarray, reverse transcription-quantitative polymerase chain reaction (RT-qPCR), annexin staining and/or bicinchoninic acid (BCA) protein analyses.

### Cell cycle analysis

Cells were grown in BFA-treated or control media for 3 days, with the media being replaced daily using freshly prepared

treated or control media. For flow cytometric cell cycle analysis the cells were trypsinized and washed twice with phosphate buffered saline (PBS) containing 0.1% FBS and subsequently fixed with −20°C ethanol by adding drop wise to the cell pellet while gently vortexing to minimize clumping. After overnight incubation at 4°C, the cells were washed twice with ice-cold PBS by centrifugation at 850*g* for 5 min, and the cell pellet was re-suspended at a final concentration of 1,000,000 cells/ml in a total volume of 300 µl. The cell suspensions then treated with 5 µg DNase-free RNase to remove all remnants of RNA and then stained with 200 µL of propidium iodide (PI; 50 µg/ml stock) prior to flow cytometry. The data were analyzed using ModFit LT software.

## *Cell death assay*

Annexin V-FITC Apoptosis Detection Kit (APOAF Sigma-Aldrich) was used to conduct an apoptosis assay on the human breast carcinoma and the human epithelial cells. After initiating apoptosis, cells translocate the membrane protein phosphatidylserine (PS) from the inner face (cytoplasmic side) of the plasma membrane to the cell surface. Once the PS is on the cell surface from the failure of flippase, it can be detected by staining with a green fluorescent protein, annexin V that has a high affinity for PS. PI was also added with this assay to detect the cells that have already undergone necrosis/cell death. Because PI enters the cell membrane of dead cells, it differentiates apoptotic from the dead cells. The MDA-MB231 and B16 cells were plated ($1 \times 10^6$) and grown in treated and control media in 60 mm plates for 3 days before performing the experiments. They were then trypsinized and removed and washed twice in PBS. The pellet of treated and control cells were then re-suspended in 500 µl of 1× binding buffer at a concentration of $1 \times 10^6$cells/ml. Then 5 µl of annexin V-FITC and 10 µl of PI were added to the cells. Due to autofluorescence, cells were ultimately analyzed with fluorescent microscopy.

## *Microarray analysis*

Replicate 60 mm dishes of either MDA-MB-231 or MCF-10A (five plates each for growth in treated and control media) were plated in DMEM-10 and the next day, the media were replaced with either treated or control media which were replaced daily with freshly prepared treated or control media for the next 2 days. On day 4 post-plating (day 3 post-treatment), the cells were removed with trypsin, counted and $3 \times 10^6$ cells from each plate were collected by centrifugation and total RNA was isolated using the RNeasy Mini Kit according to the manufacturer's instructions (Qiagen). RNA concentration was determined and RNA integrity was evaluated using an Agilent 2100 Bioanalyzer (Agilent Technologies) and all RNA integrity number (RIN) values were ⩾10. The RNAs from the five biologic replicates from each group were combined, and cDNA was generated using Ambion WT amplification kit (ThermoFisher Scientific) according to the manufacturer's instructions. The samples were subsequently fragmented and labeled using the Affymetrix WT Terminal Labeling kit and then hybridized, together with the probe array controls, onto the Human Genome U133 Plus 2.0 GeneChip Array (Affymetrix). The array was washed and stained using an Affymetrix Fluidics Station 450, scanned on an Affymetrix GCS3000 7G scanner, and the data were normalized by Robust Multichip Averaging (RMA) using the Affymetrix expression console in order to transform all the arrays to have a common distribution of intensities by removing technical variation from noisy data before analysis. To quantile normalize two or more distributions to each other, both treated and control groups were set to the average (arithmetical mean) of both distributions. Therefore, the highest value in all cases becomes the mean of the highest values, the second highest value becomes the mean of the second highest values.

## *Quantitative RT-PCR*

Ten genes which showed significant differences in expression between the treated and control MDA-MB-231 groups were chosen for validation by RT-qPCR. These included: glutathione-specific gamma-glutamyl cyclotransferase 1 (*CHAC1*), endoplasmic reticulum to nucleus signaling 1 (*ERN1*),homocysteine-inducible,endoplasmicreticulumstress-inducible, ubiquitin-like domain member 1 (HERPUD1), tumor necrosis factor receptor family 9 (*TNFRSF9*), junction-mediating and regulatory protein of p53 (*JMY*), cyclin E2 (*CCNE2*), hyaluronan-mediated motility receptor (*HMMR*), DNA-damage-inducible transcript 3 (*DDIT3*), caspase 4 (*CASP4*), and chloride intracellular channel protein 4 (*CLIC4*). Ribosomal protein S19 (*RIBOPROTS19*) was used for normalization. The primers were designed using the Universal ProbeLibrary ProbeFinder assay design software (Roche), validated and sequences are available upon request. RNAs from the five biological replicates were reverse transcribed individually using the Transcriptor First Strand cDNA Synthesis Kit (Roche) to generate cDNAs according to the manufacturer's protocol. Ten-fold serial dilutions ($10^{-1}$ to $10^{-4}$) of each of the cDNAs were then mixed with the appropriate universal library probe (UPL probe, Roche), sense and anti-sense primers, and reaction buffer into 96-well plates. The polymerase was activated by incubation at 95°C for 5 min following by a 45-cycle amplification consisting of denaturation at 95°C for 15 s, annealing at 60°C for 1 min and elongation at 72°C for 5 min.

## *Water analyses*

In order to analyze possible effects that could be occurring in the water with the BFA dc-DEP-EMF, we placed eight liters of deionized water in a 121 washbasin and 5.5 ml of 5 M NaCl were added to create a hypotonic saline solution. We then tested the solution with H2 Blue Reagent (Synergy Science) drops and conducted strip testing for total

alkalinity, pH, total hardness, stabilizer, free chlorine and total chlorine with Clorox multi-use Smart Strips (Table 3). The H2 Blue Reagent drops and the Clorox multi-use Smart Strips measure levels in ppm (1 ppm = 1 mg/l). We then placed the BFA array into the hypotonic saline solution and ran the device with dc for 35 min in the solution. The Clorox strip was placed in the water at the 34 min 30 s time point of dc application with the BFA (Table 3). We wanted to capture the levels at the end of the application and while the current was still actively being applied. At this same time point, we removed 6 ml of water from the container and placed 16 drops of the H2 Blue Reagent drops. According to the manufacturer, when one drop of the H2 is added to the solution, if this blue color turns colorless this is equivalent to 0.1 ppm (or mg/l) of H2 gas. According to the levels normally tested at atmospheric pressure and room temperature, the range in solution is 0.5–1.6 ppm. We noted that after 34 min and 30 s of exposure to the BFA-active field, the solution remained clear after 16 drops of the H2 Blue Reagent were added.

### *BCA protein analyses*

The MDA-MB231 cells were plated ($3 \times 10^6$) in two 10 cm plates and grown in treated media and control media. Media were changed daily until confluence. BCA Protein Assay Reagent Kit (Pierce 23225 23227) is a detergent-compatible formulation based on BCA for the colorimetric detection of quantitation of total protein was used for this analysis. This method utilizes a well-known reduction of copper by protein in an alkaline medium with sensitive and selective colorimetric detection of the cuprous cation. The cells were trypsinized and pelleted using 500 r/min for 5 min, then lysed in 300 µl of mammalian cell lysis buffer (Abcam ab179835). Total protein concentration was determined using the microplate procedure and the dilution parameters of 0, 200, 400, 600, 800, and 100 µg/ml were made according to the preparation of diluted albumin (BSA) standards with 50 parts of BCA Reagent A with 1 part BCA Reagent B (50:1, Reagent A: B). Once the dilutions were made, 25 µl of each standard and unknown sample replicates were pipetted into the microplate wells. Prior to placing wells in a 37°C incubator for 30 min, 200 µl of the working reagent was added to each well. The plate was then cooled to room temperature and measured at the absorbance of 562 nm on a plate reader.

### *Statistical analysis*

Cell cycle analyses were analyzed with cell flow cytometry ModFit LT, DNA cell cycle and cell proliferation software. In order to determine significant differences in percentages of cells in each cell cycle phase between the treated versus control groups, two-way analysis of variance (ANOVA) with replication and post hoc analyses with Tukey tests and unpaired t-tests were conducted. Microarray data consisted of calculated fold-change in five biological replicates of each treated and control groups in the MDA-MB-231 and MCF-10A cell lines. The microarray data were then also analyzed for top pathways, upstream and downstream regulators and targets using Qiagen's ingenuity pathway analysis (IPA, Qiagen, Redwood City, CA). RT-qPCR data were analyzed using the delta-delta CT method and unpaired t-tests. BCA protein analyses were analyzed using unpaired t-tests.

## Results

### *Cell growth*

We previously reported that the growth of the MDA-MB-231 cells was significantly inhibited when maintained in the treated media, but the MCF-10A epithelial cell lines showed no growth inhibition.[5,7] The MDA-MB-231 and MCF-10A cells were grown with the same methods employed in these growth over time analyses in order to obtain viable cells for the subsequent analyses of cell cycle microarray, RT-qPCR, annexin staining and BCA protein analyses.

### *Cell cycle analyses*

Cell cycle analyses by flow cytometry were obtained at the 3-day time point. A three-day time point was analyzed to correspond to morphological changes noted in the treated cancerous cells (i.e. increase in cell size, rounding up) that were regularly observed in our cell growth over time studies (Figure 2(e)).[5,7] Also, due to the significant growth inhibition observation in these cancerous cells, we had previously conducted tubulin staining of the MDA-MB-231 cells after 24 h of growth in treated and control media to obtain a mitotic index.[5,7] There were approximately 17% of the control MDA-MB-231 cells undergoing mitosis with 0% of the treated cells undergoing mitosis at this 24-h time point with observation of the mitotic index.[5,7] The 3-day flow cytometric cell cycle analyses were conducted at five different time points for both the treated and control MDA-MB-231 cells (Tables 1 and 5, Figure 1). We conducted a two-way ANOVA with replication analyses and found a significant interaction/effect of the BFA dc-DEP-EMF–treated growth media on the percentage of MDA-MB-231 cells measured in G0/G1 phase, S phase and G2/M phase in the treated versus control groups ($p = .016$; Tables 1 and 5; Figure 1). We then measured the flow cytometric cell cycle analyses in the percentage of MCF-10A cells measured in G0/G1 phase, S phase and G2/M phases (Tables 2 and 6). We also conducted a two-way ANOVA with replication analyses and found no significant interaction/effect of the BFA dc-DEP-EMF–treated growth media on the percentage of MCF-10A cells measured in G0/G1 phase, S phase and G2.M phase in the treated versus control groups ($p = 0.96$; Tables 2 and 6; Figure 1). Due to the significant interaction/effect noted with the two-way ANOVA of the MDA-MB-231 cells, we conducted post hoc analyses with the Tukey test and unpaired t-tests and found a

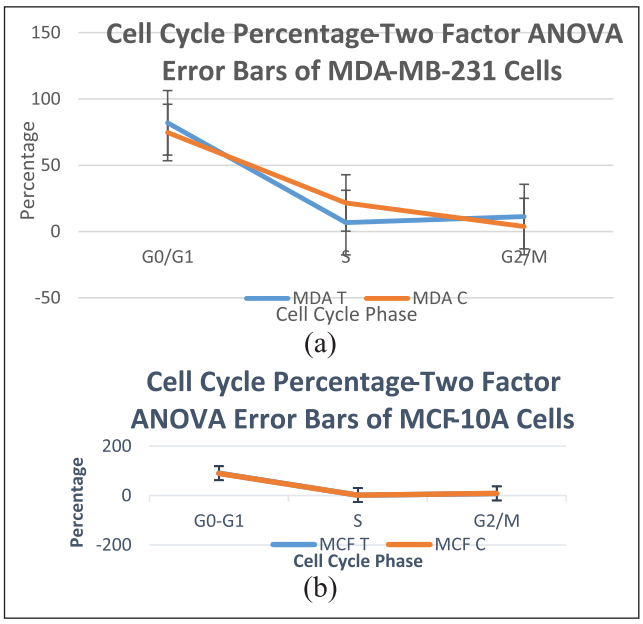


**Figure 1.** Flow cytometric cell cycle analysis of treated and control MCF-10A and MDA-MB-231 cells. Cells were grown in treated or control media for 3 days to correspond to the microarray analyses. Growth media was prepared and replaced daily prior to analyses. For cell cycle analysis, the cells were removed from the plates, fixed with −20°C ethanol and overnight incubation at 4°C. The cells were washed twice with ice-cold PBS, the cell suspensions were treated with DNase-free RNase and then stained with propidium iodide prior to analysis by flow cytometry. The data were analyzed using ModFit LT software. Two-way ANOVA with replication was run with significance at ($p < 0.05$) see ANOVA Tables 5 and 6. Data are shown in mean ± SE from five independent experiments. (a) Mean percentages and S.E. of MDA-MB-231 cells in G0-G1, S, and G2-M while maintained in either control or treated media for 3 days. (b) Mean percentages and SE of MCF-10A cells maintained in either control or treated media for 3 days. There was a significant interaction between the independent variables of treated versus control group and mean percentage of cells in the cell cycle phases in the MDA-MB-231 cells ($p = 0.016$). There was no significant interaction between the treated versus control groups and mean cell cycle percentages in the MCF-10A cells ($p = 0.99$). Post hoc analysis of the MDA-MB-231 cells with the Tukey test and unpaired t-tests show that significant difference occurs in S phase of the cell cycle (t-tests; $p = 0.04$) and ($w = 8.24$; mean difference in S phase = 14.8).

significant difference in the percentage means of the MDA-MB-231–treated versus control cells in the S phase (t-tests; $p = 0.04$; Tukey $w = 8.24$; mean difference = 14.8).

## Cell death assay

Due to the growth inhibition, cell cycle changes (Figure 1; Tables 1 and 2), and the changes in cell morphology (Figure 2(d) and (e)) in the MDA-MB-231 cells (rounding up, blebbing etc., suggestive of possible apoptosis), we conducted

**Table 1.** MDA-MB-231 percentages with cell cycle analysis by cell flow cytometry at 3-day time point and analyzed with ModFit LT.

| Cell line | G0-G1 (%) | S (%) | G2-M (%) |
|---|---|---|---|
| MDA-T | 69.92 | 0.00 | 30.08 |
| MDA-T | 72.61 | 25.27 | 2.12 |
| MDA-T | 91.73 | 8.27 | 0.00 |
| MDA-T | 85.55 | 0.00 | 14.4 |
| MDA-T | 90.10 | 0.00 | 9.90 |
| MDA-C | 87.31 | 8.77 | 3.92 |
| MDA-C | 71.20 | 28.8 | 0.00 |
| MDA-C | 73.94 | 16.83 | 9.23 |
| MDA-C | 68.36 | 25.89 | 5.75 |
| MDA-C | 72.49 | 27.51 | 0.00 |

**Table 2.** MCF-10A percentages with cell cycle analyses with cell flow cytometry at 3-day time point and analyzed with ModFit LT.

| Cell line | G0-G1 (%) | S (%) | G2-M (%) |
|---|---|---|---|
| MCF-T | 95.32 | 0.75 | 3.93 |
| MCF-T | 85.74 | 0.00 | 14.26 |
| MCF-T | 85.78 | 0.00 | 14.22 |
| MCF-T | 94.92 | 5.08 | 0.00 |
| MCF-C | 96.01 | 0.00 | 3.99 |
| MCF-C | 84.42 | 0.00 | 15.58 |
| MCF-C | 83.70 | 0.00 | 16.3 |
| MCF-C | 94.73 | 5.27 | 0.00 |
| MCF-C | 85.74 | 0.00 | 14.26 |

annexin staining via fluorescent microscopy of the MCF-10A and MDA-MB-231 cells. The human breast carcinoma MDA-MB-231 cells were positive for annexin V staining as noted by green fluorescence (Figure 2(f)), while the human breast epithelial cells remained negative for annexin V staining as noted with the absence of green fluorescence (Figure 2(c)). The positive annexin V staining in the treated human breast carcinoma (Figure 2(f)) indicated that these cells are undergoing apoptosis, while the dc-DEP-EMF–treated human breast epithelial cells (Figure 2(c)) showed no signs of apoptosis when these noncancerous cells are grown in the treated media.

## Microarray analyses

Our microarray analysis identified 1022 unique transcripts that were up or downregulated two-fold or more in the treated compared to the control media grown MDA-MB-231 cells (Figure 3(a) and (c); Supplementary Table S1). For comparison, 553 transcripts showed at least two-fold changes in expression between the treated compared to non-treated MCF-10A cells (Figure 3(b) and (d); Supplementary Table S2). Intriguingly, the magnitude of differences in the expression of select transcripts when grown in treated versus

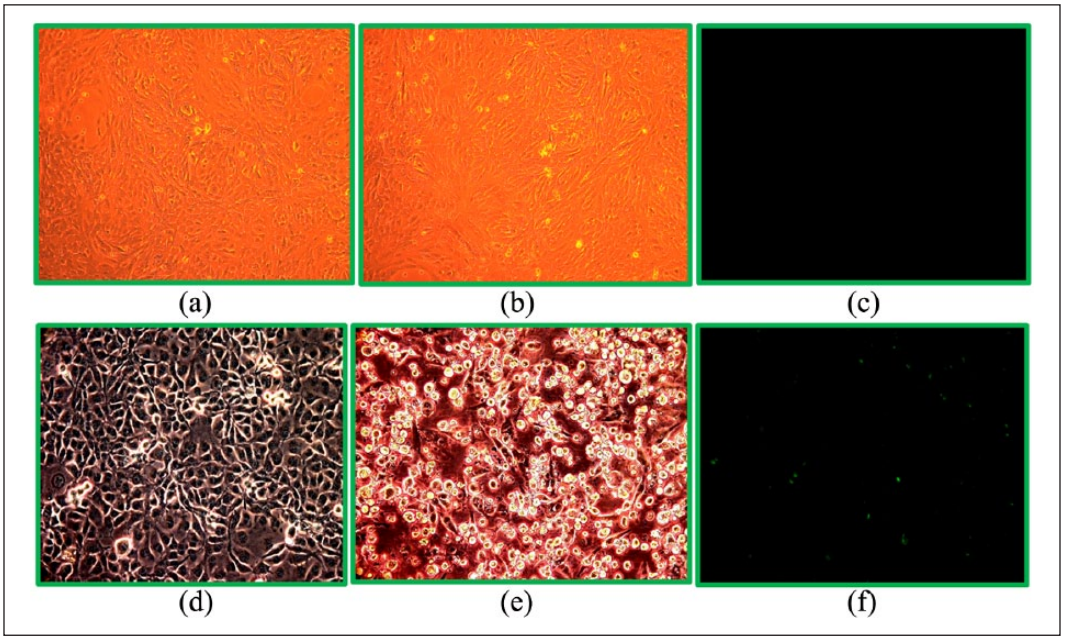


**Figure 2.** Annexin staining at day 7 of growth of the human epithelial MCF-10A cells (c) show no green fluorescence and are negative and the human breast carcinoma MDA-MB-231 cells (f) grown in treated media show green fluorescence and are positive for annexin when viewed with fluorescent microscopy. (a) MCF-10A human breast epithelial cells grown in control media, (b) MCF-10A human breast epithelial cells grown in treated media, (d) MDA-MB-231 human breast carcinoma cells grown in control media and (e) MDA-MB-231 human breast carcinoma cells grown in treated media (cells appear apoptotic). Cells were initially analyzed with cell flow cytometry to obtain percentages of cells in apoptosis, but due to the treated cells displaying autofluorescence of blue, red, green and yellow color spectrum, the green annexin staining had to be identified by fluorescent microscopy.

control media was also much greater for the MDA-MB-231 cells than the MCF-10A cells (Figure 3(c) and (d)).

Transcripts showing the most significant changes in the treated MDA-MB-231 cells included those in the ER stress and UPR pathways (Figures 3 and 4). Transcripts for *ERN1, HERPUD1, XBP1, DDIT3, CHAC1*, and *CASP4* all showed significant increases in gene expression in the MDA-MB-231 cells (Figures 3(b) and 4), which were validated using RT-qPCR (Figures 3(e) and 4). Of note, select transcripts showing the highest upregulation in the treated MDA-MB-231 cells all had the largest degree of downregulation in the treated MCF-10A cells (Figure 4), supporting the hypothesis that normal and cancer cells respond oppositely when grown in the EMF-treated media (Figure 4). These included *CHAC1* (decrease 3.35-fold), *SESN2* (decrease 2.43-fold), *FLJ46906* (decrease 2.58-fold), *ALDH1L2* (decrease 5.26-fold), and *SLC6A9* (decrease 4.65-fold). Recently, a decrease in *E2F1* expression has been shown to be required for UPR-induced apoptosis.[12] A 3.05-fold decrease in *E2F1* expression was noted in MDA-MB-231 cells grown in treated media. Transcripts for histone cluster 1 were some of the most significantly downregulated in the treated MDA-MB-231 cells, and a large number of microRNAs were differentially expressed. Interestingly, the ER stress, autophagy, and apoptosis transcripts were downregulated in the MCF-10A microarray analysis (Figure 4). Indeed, the significant genomic changes were expansive, and the implications of all these changes have not been fully investigated.

## *RT-qPCR*

The genes associated with ER stress (*ERN1, HERPUD1, XBP1, DDIT3*) were upregulated between four- to ten-fold in the treated MDA-MB-231 cells (Figures 3 and 4), suggesting that growth of this breast cancer line in the dc-DEP-EMF–treated media resulted in activation of the UPR. One effect of UPR activation is to inhibit translation and initiate cell cycle arrest.[1] *CHAC1* is a downstream regulator of the *ATF4-ATF3-DDIT3-CHOP* pro-apoptotic arm of the UPR, and *CHAC1* was upregulated 256-fold as determined by RT-qPCR in the treated MDA-MB-231 cells (Figures 3(e) and 4) and was significantly downregulated in the MCF-10A cells (Figure 4).[5,13] *CASP4*, a caspase that has been found to be associated with the UPR was upregulated four-fold in the MDA-MB-231 cells and could be an apoptotic initiator that correlates with the positive annexin staining noted in the human breast carcinoma.[14]

## *Water analysis*

In order to test for more effects in the hypotonic saline solution that could potentially be the contributing or confounding factors in these results, we measured the hardness, total chlorine,

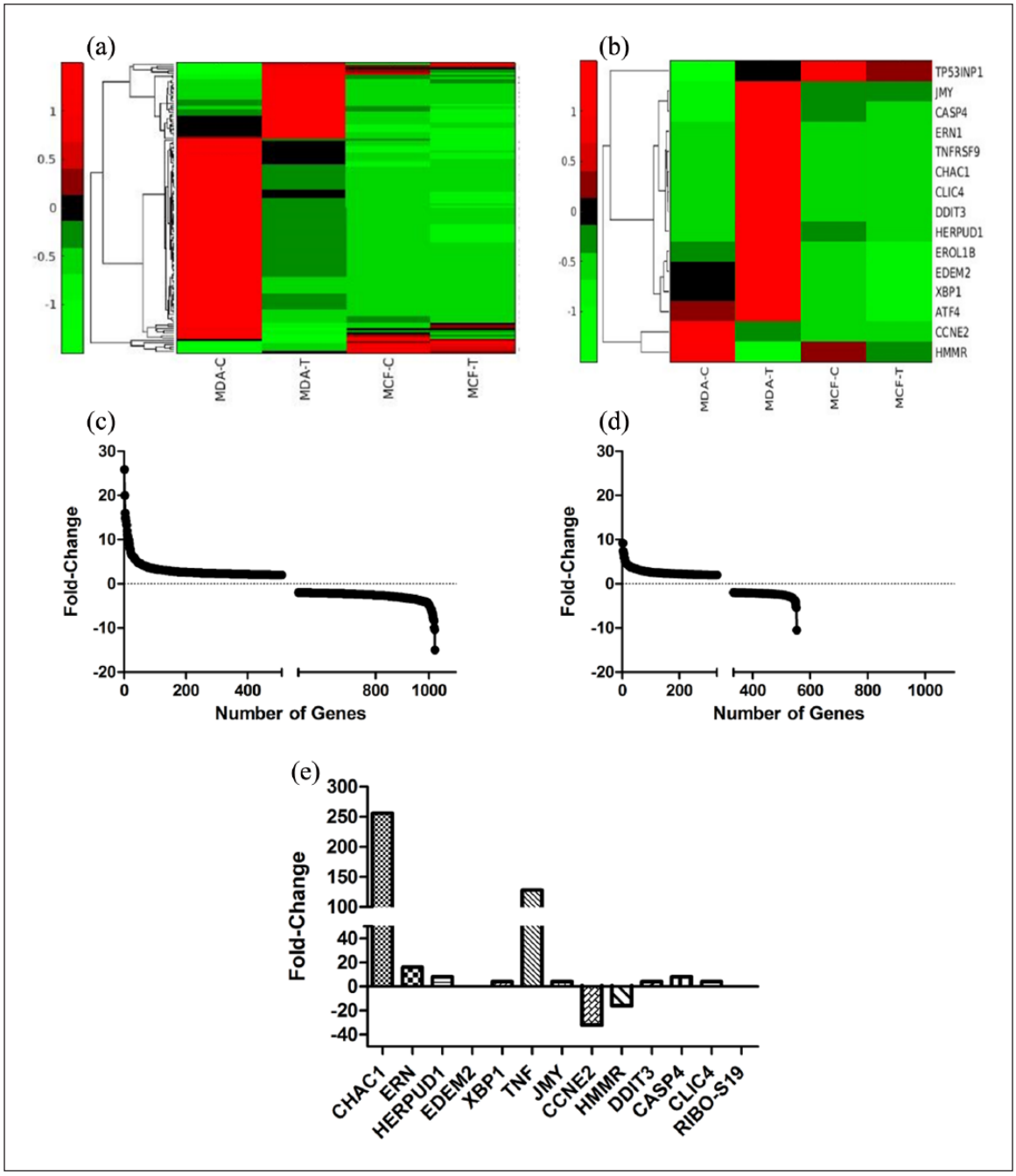


**Figure 3.** Gene expression profiling of MDA-MB-231 and MCF-10A grown in treated versus control media. (a) Five replicate plates of either MDA-MB-231 or MCF-10A were maintained in treated (T) or control (C) media for 3 days, with media changes daily. Total RNA was isolated and gene expression profiling was performed using the Affymetrix Human Genome U133 Plus 2.0 GeneChip. (b) Subset of genes from (a) involved in apoptosis and the UPR. (c) and (d), the number of unique transcripts up or downregulated two-fold or more in MDA-MB-231 (c) or MCF-10A (d) cells grown in treated versus control media for 3 days. (e) Fold-change in gene expression of select transcripts from MDA-MB-231 cells grown in treated media by RT-qPCR.

free chlorine, pH, total alkalinity, stabilizers, and molecular hydrogen (H2) in the water before and after the treatments with the BFA (Table 3). Since chlorine levels greater than 0.5 mg/l are known to be cytotoxic to cells, we wanted to determine if chlorine was produced during the dc-DEP-EMF treatment.[15] There was 0 ppm (0 mg/l) detected in treated water although there was an increase in the pH/alkalinity of the hypotonic solution after treatment with the BFA (Table 3). There was also a decrease in the hardness of the water coupled with an increase in water stability after exposure to the BFA. Finally, there was a high level of H2 detected in the hypotonic saline solution after exposure to the BFA (Table 3).

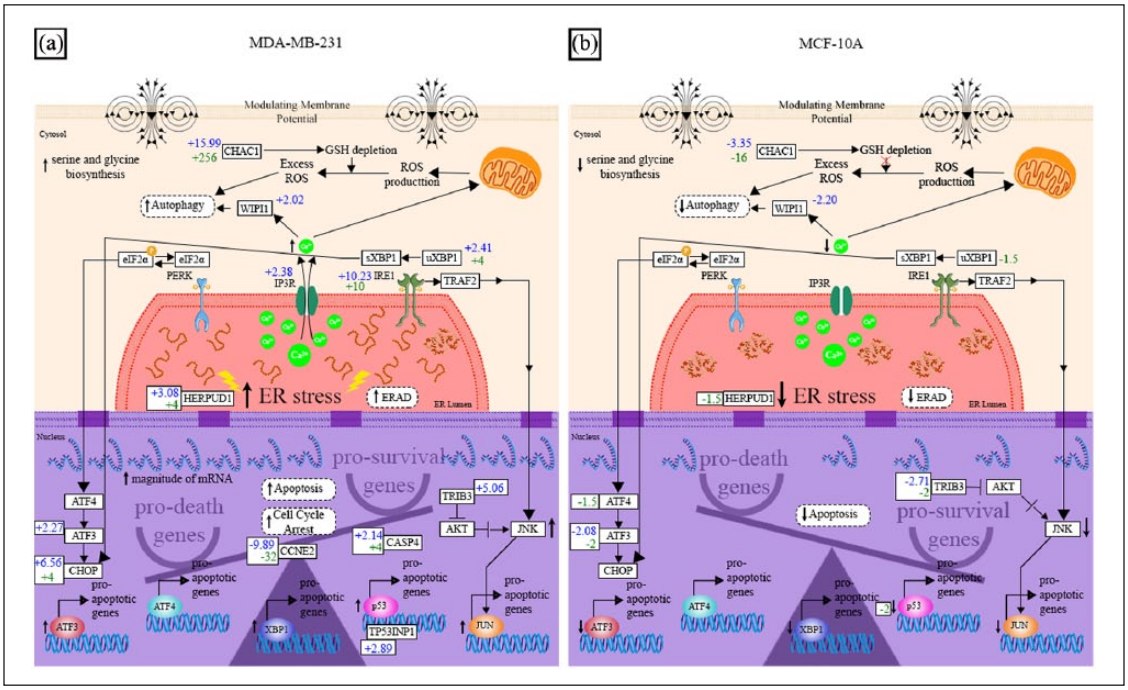


**Figure 4.** Unfolded protein response of (a) MDA-MB-231 and (b) MCF-10A cells after growth in control versus treated media. Fold-change (delta/delta CT method) with RT-qPCR (green) and microarray (blue) of control and treated (a) MDA-MB-231 (five biological replicates) and (b) MCF-10A (five biological replicates) cells. Note that the scales are heavily weighted in the pro-death gene expression of the MDA-MB-231 cells and the pro-survival genes are more heavily weighted in the MCF-10A cells. This highlights the differing responses of the cancerous (MDA-MB-231 cells) versus noncancerous (MCF-10A) cells to the BFA-dc-DEP-EMF influence, in which the apoptotic arms of the UPR are more strongly expressed in the cancer cells and the rescue/repair arms of the noncancerous cells are more strongly expressed.

**Table 3.** Hypotonic saline solution testing of hydrogen, total alkalinity, pH, total hardness, stabilizer, free chlorine and total chlorine.

| Test | Readings | | Low range | High range |
|---|---|---|---|---|
| | Before | After | | |
| H2 | 0 | 1.6 ppm | 0.5 ppm | 1.6 ppm |
| Alkalinity | 0 | 40 | 40 ppm | 240 ppm |
| pH | 6.2 | 8.4 | 6.2 | 8.4 |
| Hardness | 100 | 0 | 0 ppm | 1000 ppm |
| Stabilizer | 0 | 100 | 0 ppm | 300 ppm |
| Free/chlorine | 0 | 0 | 0 ppm | 10 ppm |
| Total/chlorine | 0 | 0 | 0 ppm | 10 ppm |

### *BCA protein analyses*

To determine if the increased transcription that was noted in the Affymetrix 2.0 gene expression analyses in the treated MDA-MB-231 cells would translate into increased total protein concentrations, we conducted a BCA protein analysis.[5,7] The BCA protein analysis showed no difference in the protein concentration at 0.2 mg/ml dilution of MDA-MB-231 cells when grown in control versus treated media for 3 days (in correlation to the microarray/RT-qPCR). Unpaired t-tests of the control mean = 0.248 and the treated mean = 0.231 resulted in no significant difference between mean protein concentrations among the two groups with $p = 0.71126$ (Figure 5).

## Discussion

MDA-MB-231 cells maintained in media prepared with dilute saline exposed to a dc-DEP-EMF generated by the BFA device resulted in significant inhibition of growth over time and significant differences (decrease) in the percentages of cells noted in S phase by flow cytometric cell cycle analyses when compared to control groups.[5] Here, we show that the growth inhibition may be due, at least in part, to a block in the G1/S phases of the cell cycle due to activation of the UPR as well as significant downregulation of multiple cell cycle regulators that showed a significant (>two-fold) downregulation in our microarray array analyses (Table 4).[16] We noted a greater than nine-fold downregulation of Cyclin E2 (*CCNE2*) in our microarray analysis and was also found to be downregulated 32-fold by RT-qPCR in the treated MDA-MB-231 cells (Figures 3 and 4). *CCNE2*, which is a regulator of CDK kinases, plays a role in cell cycle transition from G1S and *CDC25* codes for a protein required for initiation of DNA replication (S phase) which may likely be

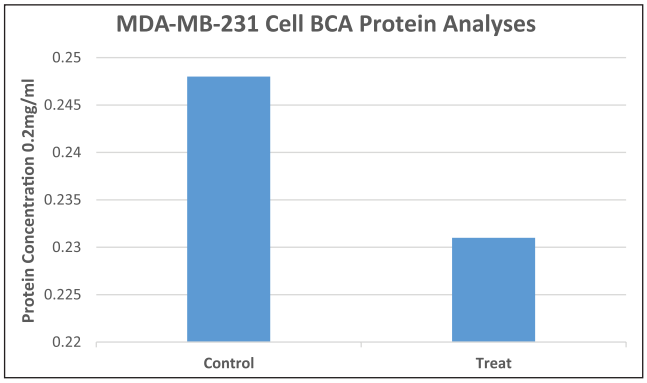


**Figure 5.** BCA protein analysis. BCA protein analysis showing difference in the protein concentration at 0.2 mg/ml dilution of MDA-MB-231 cells when grown in control and treated media for 3 days—unpaired t-tests—control mean = 0.248; treated mean = 0.231; ts = 0.380879; *df* = 10; p = 0.71126. (n = 12; n = 12; n = 12; n = 12). This shows no significant statistical difference in protein concentrations but does suggest a slight decrease in the treated protein concentration when compared to control.

**Table 4.** Affymetrix U133 Plus 2.0 microarray fold-change of cell cycle regulators in treated (vs control) MDA-MB-231 and MCF-10A cells (>two-fold = significance).

| Gene | Fold-change | |
|---|---|---|
| | MDA | MCF |
| *CCNE2* | −9.89 | −1.43 |
| *CDCA7* | −7.20 | −1.03 |
| *CDCA3* | −5.38 | −1.28 |
| *CCNA2* | −4.46 | −1.10 |
| *CDKN2C* | −4.45 | −1.12 |
| *CDC45* | −3.72 | −1.43 |
| *CDKN3* | −3.46 | −1.26 |
| *CCNB1* | −3.34 | −1.53 |
| *CDC20* | −3.32 | −1.36 |
| *CDK15* | −3.19 | −1.11 |
| *CDC25C* | −2.88 | −1.54 |
| *CDCA8* | −2.8 | −1.19 |
| *TP53INP1* | +2.88 | −1.42 |
| *CDC245A* | −2.55 | −1.12 |
| *CCNB2* | −2.37 | −1.35 |
| *CCNG1* | −2.20 | −1.21 |
| *CDCA5* | −2.09 | −1.18 |

contributing factors to the inhibitory effect on cell division and cell cycle differences observed (3 day time point; Table 5 and Figure 1) and correlates with the downregulation of histone transcripts noted in the microarray (Supplementary Table S1).[17] CDK upregulation initiates a positive feedback loop that further enhances CDK activity, thereby committing the cell to division by inducing genome-wide transcriptional changes.[18] Cyclin A2 (*CCNA2*) was also found to be downregulated over four-fold in the microarray analysis (Table 4). *CCNA2* binds and activates CDC2 or CDK2 kinases and promotes cell cycle progression through G1/S and G2/M. TP53INP1 was significantly upregulated in our microarray analysis (Table 4) in the treated MDA-MB-231 cells. TP53INP1 (Figure 4) has been shown to potentiate the capacity of p73 expression (showed a greater than two-fold increase in the treated MDA-MB-231 cells per microarray analysis) leading to cell growth inhibition, cell cycle arrest and apoptosis independent of p53.[19] Interestingly, there were also no significant change in the microarray analysis of transcripts associated with cell cycle regulation in the MCF-10A cells (Table 4).

Also, while cell growth and cell cycle of cells can be affected by the methods employed (i.e. changing growth media daily), cell growth and cell cycle phase percentage differences were only noted in the treated MDA-MB-231 versus control MDA-MB-231 but not in the growth or cell cycle of the MCF-10A cells. Both cell groups had their growth media changed daily. It is also of interest to note that there is a possible connection between cell stress and unscheduled cell cycle re-entry.[19] With the BFA dc-DEP-EMF, the cancerous cells grown in the treated media may fail to re-enter the cell cycle (S phase) while showing increased ER stress (per microarray and RT-qPCR) alternatively, the BFA dc-DEP-EMF–treated MCF-10A noncancerous cells showed an actual significant decrease in ER stress with no significant mean percentage differences in their cell cycle when compared to controls (Tables 2 and 6).[20] Cell cycle regulators have recently been noted to be intricately linked to causal and regulatory events in the development and differentiation process.[20] This novel BFA dc-DEP-EMF application shows significant downregulation of over 17 cell cycle regulators and warrants future RNA sequencing with inference of differentiation method investigations in order to provide a more detailed approach to adequately categorize these time-related events noted in these cell lines.[21]

In addition to the cell growth and cell cycle differences in the treated versus control MDA-MB-231 cells, cell morphology changes such as rounding up and blebbing were noted (suggestive of cell death) and led us to analyze the cells for possible apoptosis (Figure 2(e)). While we planned to analyze the annexin-stained cells with cell flow cytometry to obtain any percentages of cells undergoing apoptosis, autofluorescence (of the red, green yellow, and blue color spectrums) was surprisingly noted in the treated cancerous cells and prohibited the necessary differentiation of the green fluorescence in the unstained treated versus stained treated cancerous cells that is critical for this flow cytometric method. While all cells can have a natural level of fluorescence, cellular autofluorescence is known to affect the sensitivity of cell flow cytometric assays by impeding the ability to detect low level and specific fluorescence.[22] Therefore, we proceeded to analyze annexin-stained and unstained cells with fluorescent microscopy, and the green annexin was easily observed throughout the MDA-MB-231–treated stained cell

**Table 5.** Two-way ANOVA with replication for MDA-MB-231 (Figure 1(a)) treated versus control cell for flow cytometric cell cycle analysis ($p < 0.05$).

| ANOVA | SS | *df* | MS | F-stat | p-value | F-critical |
|---|---|---|---|---|---|---|
| Group | 1.33E–05 | 1 | 1.33E–05 | 1.58E–07 | 0.99 | 4.259 |
| Phase | 30563.12 | 2 | 15281.56 | 180.775 | 0.00 | 3.403 |
| Interaction | 820.699 | 2 | 410.350 | 4.854272 | 0.016 | 3.403 |
| Error | 2028.808 | 24 | 84.534 | | | |
| Total | 33412.63 | 29 | | | | |

These results would lead us to reject the $H_0$ and conclude that there was a significant effect of the BFA dc-DEP-EMF–treated growth media on the percentage of MDA-MB-231 cells measured in G0/G1, S, and G2/M in the treated versus control groups ($p = 0.016$).

**Table 6.** Two-way ANOVA with replication for MCF-10A (Figure 1(b)) treated versus control cell for flow cytometric cell cycle analysis ($p < 0.05$).

| ANOVA | SS | *df* | MS | F-stat | p-value | F-critical |
|---|---|---|---|---|---|---|
| Group | 0.000938 | 1 | 0.000938 | 2.76E–05 | 0.99 | 4.414 |
| Phase | 38803.08 | 2 | 19401.54 | 571.056 | 0.000 | 3.555 |
| Interaction | 2.617 | 2 | 1.308388 | 0.03851 | 0.96 | 3.555 |
| Error | 611.547 | 18 | 33.975 | | | |
| Total | 39417.24 | 23 | | | | |

These results would lead us to fail to reject the $H_0$ and conclude that there was not a significant effect on the BFA dc-DEP-EMF–treated growth media on the percentage of MCF-10A cells measured in G0/G1, S, and G2/M in the treated versus control groups ($p = 0.96$).

slides (Figure 2(f)) and was not noted in the treated MCF-10A or control MDA-MB-231 cells (Figure 2). This positive finding appears to correlate with the morphological microscopy changes and microarray/RT-qPCR findings as well.

As we analyzed the microarray analysis, we found that the *CLIC4* gene was upregulated approximately 2.6-fold, encodes a chloride intracellular channel that is a known participant in the stabilization of cell transmembrane potential.[5,21] *CLIC4* also has been shown to participate in suppression of tumor growth and the lack of *CLIC4* (significantly upregulated in our treated MDA-MB-231 cells) has been found to contribute to TGF-β resistance and enhanced tumor development.[21] *CLIC4* expression is linked to the novel cell sensor/mechanism of chloride ion channel modulation for these observed phenomena to date.[5] These significant changes of gene expression noted in the UPR by microarray and RT-qPCR and the other effects observed after maintenance in dc-DEP-EMF–treated media suggest that signaling events which appear to trigger induction of apoptosis in the treated human breast carcinoma cells are occurring. Alterations to cellular signaling have recently been demonstrated to occur following membrane potential induced changes to phospholipid dynamics.[23] The upregulation of *ERN1, HERPUD1, XBP1*, and *DDIT3* suggest that the human breast carcinoma cells attempted to use the rescue and repair UPR pathway to achieve homeostasis but were unsuccessful (Figures 3 and 4).[5] In addition, microarray data suggest that other indirect pro-apoptotic pathways may be affected in MDA-MB-231 cells maintained in dc-DEP-EMF–treated media. For instance, Jun N-terminal kinases (JNKs) are important mediators in death-receptor–initiated and mitochondria-initiated apoptotic pathways.[24] Our data suggest MDA-MB-231 cells can potentially activate JNK through upregulation of *ERN1-TRAF2-ASK1-MKK7-JNK* or *TRIB3-AKT-MKK4-JNK*.[11,24] This failed rescue/repair attempt then led to strong upregulation of *CHAC1* and *CTH*, both of which are involved in maintenance of glutathione levels and reducing oxidative stress in cells.[25] Also, the MCF-10A cell line showed no significant upregulation of ER stress–related transcripts with *CHAC1* (apoptosis arm of UPR) downregulated four-fold by RT-qPCR (Figure 4(b)). Because the effects of the dc-DEP-EMF treatment could be negated by high temperature and exposure to a strong magnet, our studies suggest that cells are responding to the magnetically altered ${}_bCl^-$ influence imparted by the device which induces opposing effects on normal compared to cancerous cells.[5]

Previously, we showed how the BFA dc-DEP-EMF–generated ${}_bCl^-$ has led to chemical shifts through diamagnetic anisotropy leading to cell growth inhibition, decreased migration/metastasis, membrane potential changes, modulation in chloride ion channel gene expression, increased transcription, and increased serine and glycine biosynthesis in the cancerous MDA-MB-231 cell line.[5,7] Now the BFA dc-DEP-EMF may also inhibit cell cycle progression (S phase), significantly increase ER stress, activate the pro-apoptotic arms of the UPR, and significantly increase caspase 4 (*CASP4*) expression in the MDA-MB-231 cells while significantly decreasing ER stress and not inhibiting cell cycle progression in the MCF-10A cell line (Figures 3(c) and 4).[5] Interestingly, after the noted significant increased

transcription in the treated cancerous cells, the BCA protein analyses showed no significant change in protein concentrations ($p = 0.71126$) in these cells which suggests halting of protein translation may be occurring (control mean = 0.248 mg/ml; treated mean = 0.231 mg/ml; Figure 5).[5] A reduction in protein synthesis has been found to be controlled by ER stress in plasma cells which was often preceded by a sharp enhancement in transcription.[26] Future Western blotting in in vivo models will test for significant change in any protein levels associated with these significant findings and will also help determine the BFA's ability to translate significant findings from this in vitro testing to an organism.

While these studies report that the application of a dc-DEP-EMF may influence cell growth, cell cycle ER stress, redox signaling, apoptosis, the UPR through this biotechnology's generation of ${}_bCl^-$ and molecular hydrogen (H2), and the limitations of this research to date do not make it clear if future in vitro investigations into additional cancerous and noncancerous cells lines will yield these same significant and mechanistic pathways.[27] While we can currently measure the molecular hydrogen generated by the dc-DEP-EMF during these studies, there is no current method(s) to measure the generation of the ${}_bCl^-$, and future investigations will include endeavors to measure the polarity behavioral change in this molecule. We also measured no significant increase in overall protein levels with the BCA protein analyses, and in the future, we will conduct Western blot analyses to determine if these cells are expressing individual protein levels associated with these reported pathways. Also, due to the significant changes in gene expression changes noted in the microarray, there are many more pathways and targets to investigate in order to fully understand how they all might play a role in the reported phenomena. Finally, future in vivo model testing is needed in the areas of metabolic disease, neurodegenerative disease, inflammatory disease, and cancer in order to investigate the ability to translate this work into future clinical trials.

## Conclusion

Could this dc-DEP-EMF offer a way to successfully modulate the UPR pathway by preventing cancerous cells from hijacking the rescue/repair/survival arms for their survival, while decreasing ER stress in noncancerous cells and preventing them from falling victim to apoptosis? The measured changes in pH, alkalinity, water hardness, and molecular hydrogen (H2) show possible redox potential that could, in addition to the ${}_bCl^-$ membrane modulation, contribute to the selective effects observed on the growth and transcriptional reprogramming of the MDA-MB-231 cells. There have been some similar mechanistic and redox effects in cell physiology reported with previous molecular hydrogen investigations, but chloride ion channel upregulation (${}_bCl^-$) appears to differentiate the BFA dc-DEP-EMF from these H2 applications. Also, the ability to safely modulate and control the complicated UPR pathway has been a prominent topic of research across the globe due to the potential it would create to treat multiple disease processes. This BFA dc-DEP-EMF may offer a novel quantum application (whole being) where the environment/field immediately surrounding the organism is modulated potentially offering a new intervention based in our discipline's four metaparadigms: person, environment, health, and nursing. Western medicine has its roots in pharmaceutical therapy; it may be time to bring new, noninvasive, holistic treatments to mankind. Teams of nurse scientists, in collaboration with other medical professionals, can further this research focus in hopes of finding new paths to health and wellness.

### Acknowledgements

The work was conducted in the laboratory of M.A.W., the Molecular Resource Center at UTHSC. Rita Kansal helped with technical laboratory support. E.A.T was consulted for statistical support and was a member of the dissertation committee. The authors would like to thank M.B.A.B. for his graphic design work to develop Figure 4. M.C.P. and M.A.W. conceived the research project. M.C.P., M.B.A.B., and K.B. performed experiments and analyses. All the authors contributed to writing and editing the manuscript. E.A.T. and M.C.P. edited the statistical analyses. M.A.W. was the mentor and a dissertation committee advisor.

### Animal welfare

Guidelines for humane animal treatment did not apply to this study because no animals were used for this research.

### Declaration of conflicting interests

The author(s) declared the following potential conflicts of interest with respect to the research, authorship, and/or publication of this article: Marcy C. Purnell is the co-holder of, "Bioelectrodynamics Modulation Method" United States Patent Application Publication: US 2017/0232253. Marcy C. Purnell and Michael A. Whitt. Published 8/17/2017. Marcy C. Purnell is the holder of, "Biochloride Generation and Methods" International Application Number PCT/US18/14238. Marcy C. Purnell is the holder of, "BioField Antennae and Methods of Use" International Application Number PCT/US18/26932.

### Ethical approval

Ethical approval was not sought for this study, since this study used only immortalized cells obtained from ATCC and did not require Ethics or Institutional Review Board (IRB) approval.

### Funding

The author(s) disclosed receipt of the following financial support for the research, authorship, and/or publication of this article: This works was supported by the Loewenberg College of Nursing, University of Memphis faculty grant awards; funds from the Department of Microbiology, Immunology and Biochemistry at the University of Tennessee Health Science Center; the Southern Nursing Research Society/Council of Advancement for Nursing

Science 2014–2015 National Dissertation Award; the Hal and Alma Reagan Fellowship Award, the College of Graduate Health Sciences, University of Tennessee Health Science Center 2014–2015; 2015–2016; and private donations from the Saldivar/Chisolm Families.

## ORCID iD

Marcy C Purnell https://orcid.org/0000-0002-9599-4874

## References

1. Li X, Zhang K and Li Z. Unfolded protein response in cancer: the physician's perspective. *J Hematol Oncol* 2011; 4: 8.
2. Wang S and Kaufman RJ. The impact of the unfolded protein response on human disease. *J Cell Biol* 2012; 197(7): 857–867.
3. Fulda S, Gorman AM, Hori O, et al. Cellular stress responses: cell survival and cell death. *Int J Cell Biol* 2010; 2010: 214074.
4. Corazzari M, Gagliardi M, Fimia GM, et al. Endoplasmic reticulum stress, unfolded protein response, and cancer cell fate. *Front Oncol* 2017; 7: 78.
5. Purnell MC and Skrinjar TJ. The dielectrophoretic disassociation of chloride ions and the influence on diamagnetic anisotropy in cell membranes. *Discov Med* 2016; 22(122): 257–273.
6. Purnell MC and Skrinjar TJ. Bio-electric field enhancement: the influence on membrane potential and cell migration in vitro. *Adv Wound Care* 2016; 5(12): 539–545.
7. Purnell MC. Bio-electric field enhancement: the influence on hyaluronan mediated motility receptors in human breast carcinoma. *Discov Med* 2017; 23(127): 259–267.
8. Mokrý P, Marvan M and Fousek J. Patterning of dielectric nanoparticles using dielectrophoretic forces generated by ferroelectric polydomain films. *J Appl Phys* 2010; 107: 094104.
9. Kimura T, Goto T, Shintani H, et al. Magnetic control of ferroelectric polarization. *Nature* 2003; 426(6962): 55–58.
10. Gascoyne PRC and Vykoukal J. Particle separation by dielectrophoresis. *Electrophoresis* 2002; 23(13): 1973–1983.
11. Purnell MC and Whitt MA. Bioelectrodynamics: a new patient care strategy for nursing, health, and wellness. *Holist Nurs Pract* 2016; 30(1): 4–9.
12. Pagliarini V, Giglio P, Bernardoni P, et al. Downregulation of E2F1 during ER stress is required to induce apoptosis. *J Cell Sci* 2015; 128(6): 1166–1179.
13. Mungrue IN, Pagnon J, Kohannim O, et al. CHAC1/MGC4504 is a novel proapoptotic component of the unfolded protein response, downstream of the ATF4-ATF3-CHOP cascade. *J Immunol* 2009; 182(1): 466–476.
14. Hitomi J, Katayama T, Eguchi Y, et al. Involvement of caspase-4 in endoplasmic reticulum stress-induced apoptosis and Abeta-induced cell death. *J Cell Biol* 2004; 165(3): 347–356.
15. Cervero-Aragó S, Rodríguez-Martínez S, Puertas-Bennasar A, et al. Effect of common drinking water disinfectants, chlorine and heat, on free Legionella and amoeba-associated Legionella. *PLoS One* 2015; 10(8): e0134726.
16. Pagano M, Pepperkok R, Verde F, et al. Cyclin A is required at two points in the human cell cycle. *EMBO J* 1992; 11(3): 961–971.
17. Caldon CE and Musgrove EA. Distinct and redundant functions of cyclin E1 and cyclin E2 in development and cancer. *Cell Div* 2010; 5: 2.
18. Bertoli C, Skotheim JM and de Bruin RA. Control of cell cycle transcription during G1 and S phases. *Nat Rev Mol Cell Biol* 2013; 14(8): 518–528.
19. Tomasini R, Seux M, Nowak J, et al. TP53INP1 is a novel p73 target gene that induces cell cycle arrest and cell death by modulating p73 transcriptional activity. *Oncogene* 2005; 24(55): 8093–8104.
20. Klein JA and Ackerman SL. Oxidative stress, cell cycle, and neurodegeneration. *J Clin Invest* 2003; 111(6): 785–793.
21. Suh KS, Malik M, Shukla A, et al. CLIC4 is a tumor suppressor for cutaneous squamous cell cancer. *Carcinogenesis* 2012; 33(5): 986–995.
22. Mosiman VL, Patterson BK, Canterero L, et al. Reducing cellular autofluorescence in flow cytometry: an in situ method. *Cytometry* 1997; 30(3): 151–156.
23. Zhou Y, Wong CO, Cho KJ, et al. Membrane potential modulates plasma membrane phospholipid dynamics and K-Ras signaling. *Science* 2015; 349(6250): 873–876.
24. Dhanasekaran DN and Premkumar Reddy E. JNK signaling in apoptosis. *Oncogene* 2008; 27(48): 6245–6251.
25. Crawford RR, Prescott ET, Sylvester CF, et al. Human CHAC1 protein degrades glutathione, and mRNA induction is regulated by the transcription factors ATF4 and ATF3 and a Bipartite ATF/CRE regulatory element. *J Biol Chem* 2015; 290(25): 15878–15891.
26. Goldfinger M, Shmuel M, Benhamron S, et al. Protein synthesis in plasma cells is regulated by crosstalk between endoplasmic reticulum stress and mTOR signaling. *Eur J Immunol* 2011; 41: 491–502.
27. Ohsawa I, Ishikawa M, Takahashi K, et al. Hydrogen acts as a therapeutic antioxidant by selectively reducing cytotoxic oxygen radicals. *Nat Med* 2007; 13: 688–694.